

provided sufficient aging time was allowed. We believe that these results will allow new insight into the time dependence of the domain structure in a wide variety of liquid-crystalline systems.

Acknowledgment. We thank R. M. Riddle (currently

of Texaco, Exploration and Production Research, Houston, TX) for the construction of the multinuclear accessory for the XL-100. This work was supported by the Department of Energy and the National Science Foundation.

Registry No. SHBS, 67267-95-2; aerosol OT, 577-11-7.

Coadsorbate Interactions: Sulfur and CO on Ni(100)

Marjanne C. Zonneville and Roald Hoffmann*

Department of Chemistry and Materials Science Center, Cornell University,
Ithaca, New York 14853

Received October 31, 1986. In Final Form: January 16, 1987

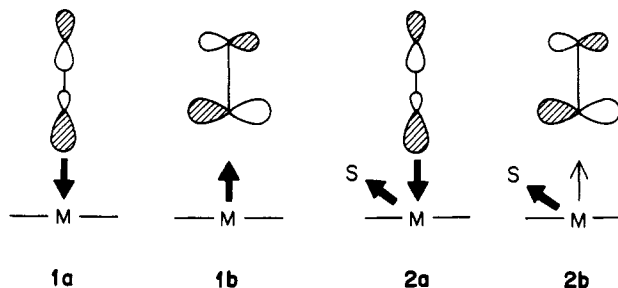
The influence of a S adlayer on CO adsorption onto Ni(100) is examined. Tight-binding extended Hückel calculations on a three-layer model slab indicate that the interadsorbate separation distance determines not only the mechanism but also the effect of the interaction. If the C-S distance is short, sulfur induces site blockage of CO chemisorption by means of a direct, repulsive interadsorbate mechanism. If the separation is increased beyond the normal S-C bond range, the sulfur adatoms work indirectly via modification of the electronic structure of the substrate. This is a form of through-bond coupling. It is consistent with the well-documented sulfur poisoning of CO adsorption and its usual explanation via relative electronegativities of adsorbates, but there are some conceptual differences. At longer coadsorbate separations, there is an interesting reversal of the bonding trends, which has some experimental support.

The effect of atomic adsorbates on the chemisorption of small molecules and on the rate of certain catalytic reactions is dramatic.¹ Electronegative impurities, such as halogens and chalcogens, tend to hinder these processes. In contrast, alkali metals and other electropositive elements can function as promoters. A great variety of experimental and theoretical studies have been conducted with the motivation of understanding the poisoning and enhancement effects of coadsorbates. For example, the adsorption of CO onto sulfided surfaces is often used as a model for the sulfur poisoning of Fisher-Tropsch hydrocarbon catalysis from CO and H₂. We will focus on S/CO coadsorbates on nickel surfaces, as the body of experimental work dedicated to these systems is voluminous.

As is true of other coadsorbate systems, the basic nature of the interactions between surface species is a matter of controversy. Opinions are substantially polarized between two extremes. The mechanism is described either as dominated by delocalized long-range effects which allow a single impurity adatom to modify many adsorption sites² or alternatively as mediated by local bonding and short-range site blockage.³ Using the army of acronymical methodologies available to surface science, experimental evidence can be found to support either side. We list only a few examples. Goodman and Kiskinova^{2,4} and Erley and Wagner⁵ advocate the long-range theory based on the well-documented nonlinearity of both the CO saturation coverage and CO/H₂ catalytic methanation as a function of preadsorbed sulfur on Ni(100) and Ni(111). On Ni(100), a one-fifth sulfur monolayer causes an order of magnitude decrease in the rate of methanation. Goodman⁶ concludes

that each sulfur atom affects some 10 Ni surface atoms. Madix et al.^{3,7,8} implicate local site blockage to explain similar results. Gland et al.⁹ favor the short-range model for Ni(100) in light of high-resolution electron energy loss spectroscopy (HREELS) and temperature-programmed desorption (TPD) studies. The infrared reflection-adsorption spectroscopy (IRAS) work of Trenary et al.¹⁰ on Ni(111) is in good agreement with the latter.

Theoretical treatments of adatom poisoning and promotion of CO chemisorption are generally presented in the framework of the Blyholder model.¹¹ The adsorption geometry is widely accepted to be through the carbon end, exactly or nearly perpendicular to either the clean or preadsorbed nickel surface.^{12a-d} Regardless of the specific adsorption site, the chemisorptive bond in the Blyholder model results from the electron donation from the CO 5σ, 1a, into the empty surface levels and back-donation from the surface into the CO 2π*, 1b. As both CO levels are



(7) Madix, R. J.; Thornburg, M.; Lee, S. B. *Surf. Sci.* **1983**, *133*, L447.

(8) Madix, R. J.; Lee, S. B.; Thornburg, M. *J. Vac. Sci. Technol. A* **1983**, *1*, 1254.

(9) Gland, J. L.; Madix, R. J.; McCabe, R. W.; DeMaggio, C. *Surf. Sci.* **1984**, *143*, 46.

(10) Trenary, M.; Uram, K. J.; Yates, J. T., Jr. *Surf. Sci.* **1985**, *157*, 512.

(11) Blyholder, G. *J. Phys. Chem.* **1964**, *68*, 2772.

(12) (a) Behm, R. J.; Ertl, G.; Penka, V. *Surf. Sci.* **1985**, *160*, 387 and references therein. (b) Allyn, C.; Gustafsson, T.; Plummer, E. *Solid State Commun.* **1978**, *23*, 85. (c) Andersson, S.; Pendry, J. B. *Phys. Rev. Lett.* **1979**, *43*, 363. (d) Passler, M.; Ignatiev, A.; Jona, F.; Jepsen, D. W.; Marcus, P. M. *Phys. Rev. Lett.* **1979**, *43*, 360.

(1) For recent reviews on poisoning and promotion, see: (a) Martin, G. A. In *Metal Support and Metal-Additive Effects in Catalysis*; Imelik, B., et al., Eds.; Elsevier: Amsterdam, 1982; p 315. (b) Goodman, D. W. "Role of Promoters and Poisons in CO Hydrogenation" In *Proc. IUCCP Symp.*, TX, 1984.

(2) Goodman, D. W.; Kiskinova, M. *Surf. Sci.* **1981**, *108*, 64.

(3) Johnson, S.; Madix, R. J. *Surf. Sci.* **1981**, *108*, 77.

(4) Goodman, D. W.; Kiskinova, M. *Surf. Sci.* **1981**, *105*, L265.

(5) Erley, W.; Wagner, H. *J. Catal.* **1978**, *53*, 287.

(6) Goodman, D. W. *Appl. Surf. Sci.* **1983**, *19*, 1.

localized on the carbon end,¹³ they are at least geometrically well suited for the electron transfers. Sulfur and other electronegative adatoms withdraw electron density from the surface. Little change in 5σ to metal donation, **2a**, is presumed, but metal to $2\pi^*$ back-bonding, **2b**, should be reduced, and hence the poisoning effect. As the occupation of the C–O antibonding $2\pi^*$ decreases, the C–O bond strengthens at the expense of the chemisorptive bond. Electropositive adatoms should work in the opposite manner. Electron density is pushed into the surface, thus enhancing its back-bonding capacity.

Theoretical studies are able to reproduce poisoning and promotion and most indicate, at minimum, a rudimentary agreement with this simple MO picture. A cornucopia of calculation methodologies has been called upon, including LCAO type on clusters^{14a–f} and monolayers,¹⁵ monolayer SLAPW type,¹⁶ cluster LCGTO- $X\alpha$,^{17a,b} the effective-medium theory applied to jellium surfaces,^{18a,b} the muffin-tin approximation applied to clusters,¹⁹ and, most recently, all-electron local-density-functional theory.²⁰ Nevertheless, there is no more agreement (as to the range or detailed nature of the interactions) between the various calculations than that found in experimental studies. Benzinger and Madix¹⁵ suggest that direct interadsorbate interactions may be the key factor, although the metal-mediated electron transfers predicted from the Blyholder mechanism are clearly reproduced. On the other hand, Nørskov et al.^{18a,b} find long-range electrostatic forces to be more significant. The FLAPW results of Wimmer et al.²⁰ straddle the controversy. A long-range interaction is dominant for a K adatom, but for S, both direct and substrate-mediated effects are surmised.

In this paper, we examine the S + CO system on Ni(100) with the extended Hückel tight-binding method.^{21a,b} The procedure is an approximate MO method with well-known deficiencies. It does not give reliable potential energy curves or binding energies, nor is it able to properly model magnetism. The work function and ionization potentials are quite far from the true values. But it is a transparent methodology and reveals clearly the basic interactions that are responsible for bonding. The calculations we report are for nonmagnetic, spin-paired metal and adsorbate.

We will assemble the Ni/S/CO system from its various component parts. Computational details are given in the Appendix. As the focus of previous work by this group has been the adsorption of CO onto Ni(100) and other surfaces,²² several of the closely related systems—the bare Ni(100) surface, the unadsorbed CO net, the Ni(100)- $c(2 \times 2)$ CO on top and Ni(111)CO bridging—are well characterized and our discussion will be appropriately brief.

For the Ni(100) substrate, a three-layer slab with the bulk nickel lattice constant ($a = 3.524 \text{ \AA}^{23}$) was used. The nearest-neighbor contact is 2.49 Å on this square net surface. The calculated density of states (DOS) exhibits a compact d band between -12 and -8 eV and very dispersed s and p bands between -12 and 8 eV .^{22,24} As the surface atoms have a lower coordination number, these states are less dispersed than the bulk states. Consequently, if the Fermi level falls above the midpoint of the d block, as for nickel, the surface is negatively charged with respect to the bulk.

Whether the three-layer slab is an appropriate model for the surface can be estimated from the charge on the middle layer. An infinitely deep system will have a bulk charge approaching zero. With a 55K point set,²⁵ we compute an excess charge of $+0.180e^-$ per atom for three layers, $+0.166e^-$ for four layers, and $+0.157e^-$ (middle layer) for five. As the convergence is slow in this range of reasonably sized unit cells, we make our choice on the basis of computational economics. The three-layer substrate was used for all calculations.

Our first priority in the study of the S/CO system on Ni(100) is to establish proper adsorption geometries. So let us review briefly what is known from experiment. The preference for atomic adsorption at the highest coordination site is nearly universal on clean or coadsorbed transition-metal surfaces.²⁶ Specifically, chalcogen adsorption at the Ni(100) four-fold hollow is well documented.^{27a–e} CO chemisorbs molecularly and does not dissociate to any measurable degree on late-transition-metal surfaces.²⁸ On clean Ni(100), CO site preference is coverage and temperature dependent.^{29a–c} At saturation coverage and below 150 K, a compression structure of both on-top and bridging CO is formed. When the compression structure is relaxed to a $\theta = 0.5$, $c(2 \times 2)$ monolayer (or if coverage is further reduced), only the on-top mode is observed. The HREELS vibrational spectrum⁹ is characterized by a single C–O stretching frequency at 2005 cm^{-1} . If sulfur is added, and its surface concentration is increased, this dominant peak is down-shifted and two new CO modes grow in, one at a lower frequency and the other at a higher frequency. The adsorption geometry of the new modes is unknown. Using partial thermal desorption, the high-frequency peak is correlated to low-temperature desorption, the low-frequency peak to high temperature, and the dominant mode to an intermediate temperature. The CO layer is completely desorbed below 430 K, which is the predominant desorption temperature from the clean surface. The inverse relationship between the C–O stretch frequency and desorption temperature is consistent with the greater susceptibility of the chemisorptive bond strength to the π rather than the σ system, as advocated in the Blyholder mechanism. However, we expect a unidirectional effect;

(13) For the MO's of CO, see: Jorgensen, W. L.; Salem, L. *The Organic Chemist's Book of Orbitals*; Academic: New York, 1973; p 78.

(14) (a) Ray, N. K.; Anderson, A. B. *Surf. Sci.* **1983**, *125*, 803. (b) Ray, N. K.; Anderson, A. B. *Surf. Sci.* **1982**, *119*, 35. (c) Anderson, A. B.; *Surf. Sci.* **1977**, *62*, 119. (d) Tománek, D.; Bennemann, K. H. *Surf. Sci.* **1983**, *127*, L111. (e) Cao, P.-L.; Shi, D.-H. *Acta Phys. Sin.* **1985**, *34*, 1291. (f) Rodriguez, J. A.; Campbell, C. T., unpublished results.

(15) Benzinger, J.; Madix, R. J. *Surf. Sci.* **1980**, *94*, 119.

(16) Feibelman, P. J.; Hamann, D. R. *Phys. Rev. Lett.* **1984**, *52*, 61.

(17) (a) Dunlap, B. I.; Yu, H. L.; Antoniewicz, P. R. *Phys. Rev. A* **1981**, *25*, 7. (b) Jörg, H.; Rösch, N. *Surf. Sci.* **1985**, *163*, L627.

(18) (a) Nørskov, J. K.; Holloway, S.; Lang, N. D. *Surf. Sci.* **1984**, *137*, 65. (b) Lang, N. D.; Holloway, S.; Nørskov, J. K. *Surf. Sci.* **1985**, *150*, 24.

(19) MacLaren, J. M.; Pendrey, J.; Vvedensky, D. D. *Surf. Sci.* **1985**, *162*, 322.

(20) Wimmer, E.; Fu, C. L.; Freeman, A. J. *Phys. Rev. Lett.* **1985**, *55*, 2618.

(21) (a) Hoffmann, R. *J. Chem. Phys.* **1963**, *39*, 1397. Hoffmann, R.; Lipscomb, W. M. *Ibid.* **1962**, *36*, 3179; *Ibid.* **1962**, *37*, 2872. (b) Ammeter, J. H.; Bürgi, H.-B.; Thibeault, J. C.; Hoffmann, R. *J. Am. Chem. Soc.* **1978**, *100*, 3686.

(22) Sung, S.-S.; Hoffmann, R. *J. Am. Chem. Soc.* **1985**, *107*, 578.

(23) Donohue, J. *The Structure of the Elements*; R. E. Kreiger: Malabar, FL, 1982.

(24) Saillard, J.-Y.; Hoffmann, R. *J. Am. Chem. Soc.* **1984**, *106*, 2006.

(25) Pack, J. D.; Monkhorst, H. J. *Phys. Rev. B* **1977**, *16*, 1748.

(26) For example, see: van Hove, M. A. In *The Nature of the Surface Chemical Bond*; Rhodin, T. N.; Ertl, G., Eds.; North-Holland: Amsterdam, 1979; p 277.

(27) (a) Fisher, G. B. *Surf. Sci.* **1977**, *62*, 31. (b) Perdureau, M.; Oudar, J. *Surf. Sci.* **1970**, *20*, 80. (c) Demuth, J. E.; Jepsen, D. W.; Marcus, P. M. *Phys. Rev. Lett.* **1973**, *31*, 540. (d) Andersson, S. *Surf. Sci.* **1979**, *79*, 385. (e) Hagstrum, H. D.; Becker, G. E. *J. Chem. Phys.* **1971**, *54*, 1015; *Phys. Rev. Lett.* **1969**, *22*, 1054.

(28) Brodén, G.; Rhodin, T. N.; Brucker, C. F.; Benbow, R.; Hurych, Z. *Surf. Sci.* **1976**, *59*, 593.

(29) (a) Andersson, S. *Solid State Commun.* **1977**, *21*, 75. (b) Andersson, S. In *Proceedings of the 7th International Vacuum Congress & 3rd International Conference on Solid Surfaces*; Vienna, 1977; p 1019. (c) Mitchell, G. E.; Gland, J. L.; White, J. M. *Surf. Sci.* **1977**, *62*, 31.

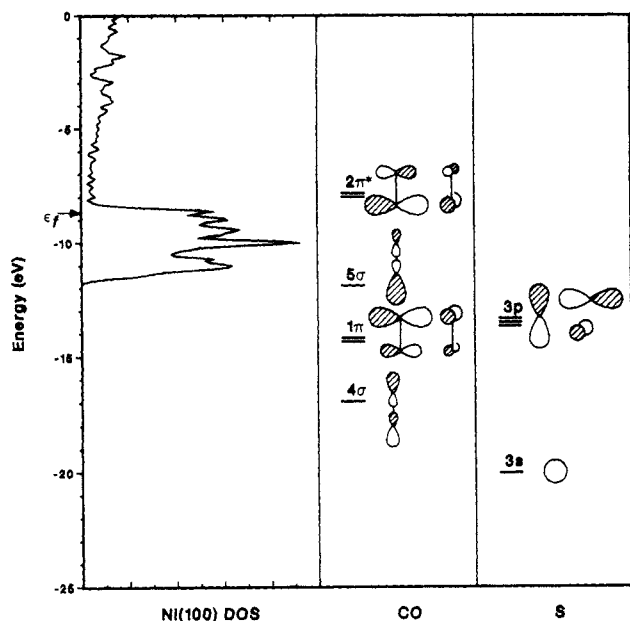


Figure 1. In the left panel, the bare Ni(100) DOS. The valence orbitals of CO and S are drawn in the middle and right panels, respectively.

the sulfur should reduce π -back-bonding. The C-O bond strengthens as the chemisorptive bond weakens, thereby creating a high CO frequency, low desorption temperature mode. Although two such modes are observed, a third, apparently originating from increased π -back-bonding, does as well. We ambitiously hope to model these results by examining the effect of sulfur coadsorption on the binding of CO at various sites and, as well, gain general insight into the mechanism of coadsorbate interactions.

In the case of the adsorbed systems, we retained the Ni bulk geometry for the three-layer substrate slab. (2×2) chalcogenide overlayers do not cause reconstruction of this surface; however, relaxation must be considered. For the clean Ni(100) surface, the spacing between the first and second layers is estimated to be contracted by 3%, based on ion blocking measurements.³⁰ EELS studies indicate that no further relaxation occurs for (2×2) S adlayers.³¹ To our knowledge, it is not known whether reconstruction or relaxation occur in the presence of both S and CO. While the geometric changes are not insignificant, they are not included in our calculations.

A coverage of $\theta = 0.25$, $p(2 \times 2)$, per adsorbate species was chosen. It is in this coverage range that the three C-O stretch peaks first appear simultaneously in the HREELS spectra.⁹ Each species is laid out in a square net, lattice constant $a = 4.98 \text{ \AA}$. The calculated band structures of CO²² and S unsupported nets are essentially free of dispersion. The band energies are equivalent to the molecular orbital energies, thus intraspecies interactions are negligible at this distance. To help us see the important orbitals of both adsorbates and their relative energies, we show in Figure 1 the total density of states (DOS) of the bare Ni slab and, alongside, the important frontier orbitals of S and CO.

One of the prerequisites for the electronegativity arguments concerning poisoning is that the electron-withdrawing power of sulfur be observed in Ni(100)- $p(2 \times 2)$ S, that is, without CO coadsorption. K point sets of 10

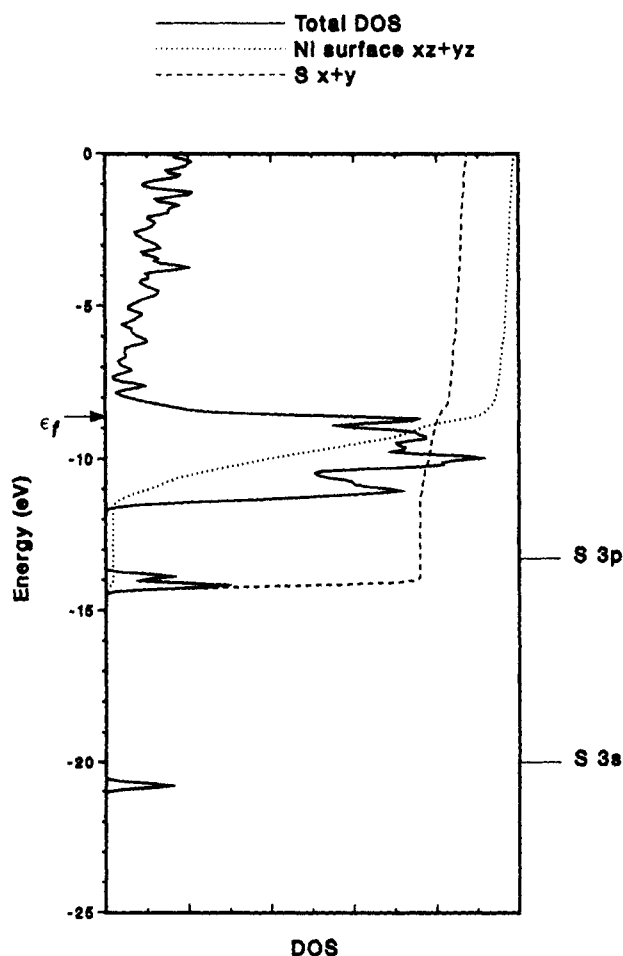
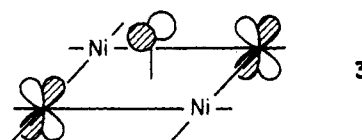


Figure 2. Solid line indicates the Ni(100)- $p(2 \times 2)$ S total DOS. The dotted and dashed lines are the integrals of the surface $xz + yz$ and $Sx + y$ projected DOS, respectively. The S unsupported square net DOS is represented by the median energy bars on the right.

and 16 were used for substrate plus adsorbate(s) systems with tetragonal and orthorhombic symmetry, respectively (see Appendix for calculations testing convergence). The sulfur square net is placed on the substrate such that S occupies 4-fold hollow sites and $d(\text{S-Ni}) = 2.19 \text{ \AA}$,³² as obtained from LEED. The z axis is consistently oriented perpendicular to the Ni plane, and the x and y axes are parallel to the surface Ni-Ni close contacts. The charge transfer occurs as predicted; the sulfur adatoms gain $0.756e^-$, and each of the four associated surface atoms loses $0.355e^-$ relative to bare Ni(100). Although the charge transfer is greatest in the nickel xz and yz ($-0.115e^-$ each) and the sulfur z levels ($+0.481e^-$),³³ the projected DOS indicate that the strongest interaction is with the sulfur x and y rather than z levels. The p band of the S square net lies at -13.2 eV , well below both the d block and the Fermi energy of the bare substrate (-8.7 eV). The large dispersion provided by the interactions with surface xz and yz states, such as the representative one depicted in 3,



(30) Frenken, J. W. M.; Smeek, R. G.; van der Veen, J. F. *Surf. Sci.* **1983**, *135*, 147. Frenken, J. W. M.; van der Veen, J. F.; Allan, G. *Phys. Rev. Lett.* **1983**, *51*, 1876.

(31) Lehwald, S.; Rocca, M.; Ibach, H.; Rahman, T. S. *J. Electron Spectrosc. Relat. Phenom.* **1986**, *38*, 29.

(32) Reference 26, p 292.

(33) The reference occupation for sulfur atomic orbitals is $2e^-$ for s and $1.333e^-$ for each p .

forces some 20% of the S x and y states above the Fermi energy and splits the major S x and y peak down from the z peak by ~ 0.5 eV. Some surface xz and yz character appears in the S x and y peak near -14 eV, as seen in a comparison of the projected DOS integration curves in Figure 2. In contrast, the S z level acts essentially as an inert electron sink.

The total DOS (solid line in Figure 2) appears very much as a simple overlay of the S square net DOS (represented schematically on the right by bars at the median energies) and the bare Ni(100) DOS.²⁶ The binding energies of the sulfur p and s levels agree with those obtained by UPS^{27a} within experimental error. The S adlayer is a relatively small perturbation on the electronic structure of the Ni(100) slab as a whole but does cause substantial charge redistribution and rehybridization at a local level. If poisoning does occur via the substrate, the xz and yz surface levels are the most likely mediators.

We consider three high-symmetry sites for CO coordination: on top, bridging, and four-fold hollow. The C-Ni and C-O bond lengths are determined by LEED as 1.80 and 1.15 Å, respectively,^{12c} for on-top coordination, the only one known to exist independently. In general, our computational method cannot be trusted to predict the energetics of adsorbate site preference. So we must make some geometric choices. For the bridging and 4-fold sites, all calculations on both clean and sulfur-coadsorbed surfaces were performed at two limiting geometries: C-Ni nearest-neighbor distance of 1.80 Å and C-Ni surface distance of 1.80 Å. The trends are identical but consistently more pronounced for the first option, which we choose to present for the sake of clarity.

Characteristic of the rather weak chemisorption of CO onto nickel and other late transition metals, the CO molecular levels for the observed on-top geometry form bands which have a small dispersion and are at nearly the same energy as the molecular levels. In contrast, one-third of the bridging and 4-fold $2\pi^*$ levels are pulled into the d block. Specific features of the DOS will be discussed later, in conjunction with the coadsorbed systems.

Our models adhere closely to the Blyholder model of σ -donation and π -back-donation. The electron density shifts from bare Ni(100) or molecular CO to Ni(100)- $p(2 \times 2)$ CO are presented in Table I. The extent of 5σ depopulation falls within a much narrower range than does the amount of back-donation into $2\pi^*$.^{34a,b} The σ interaction contributes to the net bonding in a relatively uniform manner for all sites. On the other hand, the C-O overlap population (op) follows the $2\pi^*$ occupation exactly as predicted. Moving through the coordination series of molecular, on top, bridging and 4-fold, the C-O op falls in conjunction with growing $2\pi^*$ occupation. The CO coordination number mediates the electronic shifts at the associated surface atoms, the largest shift coincides with the lowest coordination. The average electron loss, however, correlates well with the gain in $2\pi^*$ but is independent of 5σ . These two effects underlie the notion that the chemisorptive interaction is governed by the extent of π -back-bonding against a fairly uniform σ -donation background. Unfortunately, we cannot compare the strengths of the chemisorptive bonds directly; the effect of coordination number on overlap population is generally nonlinear.

Table I. Calculated Results for Ni(100)- $p(2 \times 2)$ CO

atom(s) or orbitals	CO coordination mode		
	on top	4-fold	bridging
Electron Density Changes ^a			
CO total	+0.249	+0.777	+0.638
CO 5σ	-0.379	-0.368	-0.398
CO $2\pi^*$ ^b	+0.372	+0.694	+0.598
Ni _s , coordinated	-0.814	-0.283	-0.542
Ni _s , uncoordinated	-0.005		-0.002
Ni _s , average	-0.200	-0.283	-0.273
Overlap Populations			
C-O ^c	1.044	0.916	0.942
C-Ni _s	0.847	0.359	0.631
CO binding E , eV ^d	+2.570	+2.526	+3.843

^aRelative to Ni(100) or molecular CO. Net electron gain if positive, loss if negative. ^bOccupation of $2\pi^*$ and other degenerate orbitals are given for each individual orbital. ^cMolecular C-O $op = 1.208$. ^d $E(\text{Ni(100)}) + E(\text{molecular CO}) - E(\text{Ni(100)-}p(2 \times 2) \text{ CO})$.

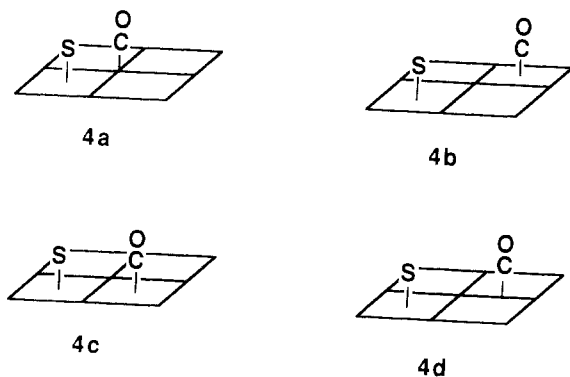
Atomic electron transfers must, however, be used with care. In this case, both CO interactions work to decrease the surface electron density. Most of the d block lies just below the Fermi energy so that some states will be pushed above it by dispersion from any source, whether from below (5σ) or above ($2\pi^*$).²² That d -block states can be raised above ϵ_f by interaction with $2\pi^*$ merits a word of discussion. Very simplistically, mixing between a fully occupied "d" and empty " $2\pi^*$ " states will create a " $d + \lambda 2\pi^*$ " state below ϵ_f and a " $2\pi^* - \lambda d$ " state above ϵ_f (λ is an arbitrary mixing parameter). The net charge transfer will be out of d and into $2\pi^*$. Although the bare-surface d -block occupation is actually $9.3e^-$ rather than $10.0e^-$, it is not hard to imagine that simply by their preponderance, the occupied states will dominate. The two effects are most cleanly separated at the on-top geometry. The orbitals able to interact with the 5σ do not interact effectively with the $2\pi^*$, and vice versa. The appropriate surface d orbitals (z^2 for 5σ , xz and yz for $2\pi^*$) experience nearly identical charge shifts. Since the 5σ occupation is very similar at the three sites, we can safely surmise that its interaction with the substrate is constant and the total surface electron loss is determined by the $2\pi^*$.

With regard to the electronegativity arguments concerning sulfur poisoning, we suggest that the electron-withdrawing power of CO must be considered as well. The total charge transfer into CO is approximately one-third of that into the S of Ni(100)- $p(2 \times 2)$ S for CO on top but nearly equivalent for the bridging and 4-fold coordinations. Although the point must be reconsidered for the coadsorbed systems, this result makes rationalizations based on electronegativity alone less self-evident.

Four Ni(100)- $p(2 \times 2)$ S + $p(2 \times 2)$ CO systems have been considered: (1) CO on top, **4a**, (2) CO in 4-fold hollow retaining tetragonal symmetry (4-fold tetra), **4b**; (3) CO in 4-fold hollow, symmetry reduced to orthorhombic (4-fold ortho), **4c**; and (4) CO bridging, **4d**. The top layer of the three-layer unit cell is shown in the schematics. In each case, we have left the S in a four-fold hollow. Behind this assumption is the strong propensity of the S for this site; to our knowledge, no deviation from such adsorption is known experimentally. CO, on the other hand, is known to have low barriers to moving into alternative coordination modes.

The evolution of the C-O and C-Ni_s op 's (Ni_s = surface atom) upon sulfur coadsorption, shown in Table II, is intriguing in light of the Blyholder and "anti-Blyholder" modes observed by Gland.⁹ Just as predicted by the Blyholder mechanism, S coadsorption in the 4-fold ortho,

(34) (a) Bagus, P. S.; Nelin, C. J.; Bauschlicher, C. W., Jr. *J. Vacuum Sci. Technol. A* 1984, 2, 905. (b) Bauschlicher, C. W., Jr.; Bagus, P. S. *J. Chem. Phys.* 1984, 81, 5889. These workers seem to conclude that the net σ interaction contributes little to the chemisorptive bond, with which we are not in agreement.



4c, and bridging, 4d, systems induces C–O bond strengthening and C–Ni_s bond weakening and reduces the CO binding energy. Although the absolute binding energies calculated by the extended Hückel method are unreliable and we are unable to predict adsorption site preferences, the relative binding energies at the same site can be used with more confidence. We tentatively associate the 4-fold ortho and bridging sites with the high-frequency C–O stretch, low-temperature desorption mode. Exactly the opposite effects are observed for the 4-fold tetra, 4b. This site corresponds to the “anti-Blyholder” low-frequency C–O stretch, high-desorption-temperature mode. That the interaction between adsorbates is nonisotopic is not without precedence. Other workers^{35a,b} have proposed that the interaction is an oscillatory function of the separation distance, thus alternately repulsive or attractive.

Both bonds are weakened if CO is bound on top, and the CO binding energy decreases so sharply that the Ni(100)– $p(2 \times 2)$ S + $p(2 \times 2)$ CO system is less stable than its separated components. The anomalous behavior arises directly from the close C–S contact. In this geometry, 4a, with $1/4$ coverage for both S and CO, the S–C(O) separation is only 1.83 Å. This is very much within a bonding range; indeed typical S–C single bonds fall between 1.75 and 1.80 Å. The computed C–S op is 0.627, which is the largest value of any site (the bridging mode is a distant second at 0.015). The surface species is better described as molecular SCO than as coadsorbed S and CO. To our knowledge, no evidence of SCO formation has been observed for any coadsorbed S/CO surface. The energy of this coadsorbate geometry is very high. We believe it is energetically inaccessible and that what we are in fact modeling is local site blockage.

Essentially all other calculations to date have been performed at similarly short C–S contacts. This distance is crucial; at 1.83 Å we observe site blockage, at 2.66 Å (4-fold ortho) and 2.78 Å (bridging) the Blyholder result, and at 3.64 Å (4-fold tetra) an “anti-Blyholder” effect. The smallest distance must be classified as short-range and the large S–C op strongly indicates a direct interadsorbate effect; the largest is clearly long-range and its corresponding op is negligible (–0.003), pointing to a surface-mediated interaction. The problem, then, may not be to determine the absolute range of interadsorbate interactions but rather to identify the type of interaction active in each range.

An important point in our analysis is that the $2\pi^*$ occupation follows the strength of the chemisorptive bond. The trends shown in Table III are consistent with the π -back-bonding mechanism; invariably C–Ni_s op reduction is coincident with $2\pi^*$ depopulation, and vice versa.

The relative electron-withdrawing power of the two adsorbates is reconsidered in Table IV. Relative charge transfer is defined as the atomic electron density in Ni-

Table II. Overlap Populations and Binding Energies

CO site	C–O overlap population		C–Ni _s overlap population		Δ CO binding E , eV ^a
	without S	with S	without S	with S	
on top, 4a	1.044	0.929	0.847	0.579	+3.391
4-fold tetra, 4b	0.916	0.906	0.359	0.363	–0.050
4-fold ortho, 4c	0.916	0.928	0.359	0.336	+2.435
bridging, 4d	0.942	0.974	0.631	0.581	+1.256

^a (CO binding E with S) – (CO binding E without S).

Table III. Occupation of $2\pi^*$

CO site	predicted change ^a	occupation	
		without S	with S
on top	–	0.372	0.515
4-fold tetra	+	0.694	0.717
4-fold ortho	–	0.694	0.686
bridging	–	0.598	0.521

^a Based on C–Ni_s overlap population trends.

Table IV. Electron Transfer to Coadsorbates Relative to Single-Species Systems^a

CO site	S	CO
on top, 4a	–0.530	–0.009
4-fold tetra, 4b	+0.015	+0.071
4-fold ortho, 4c	–0.041	–0.050
bridging, 4d	–0.051	–0.179

^a A positive value indicates an electron density gain relative to single-species adsorption and a negative value, an electron loss.

Table V. Electron Density Changes,^a Bridging CO

atom(s) or orbitals	Ni(100)– $p(2 \times 2)$ CO rel to Ni(100) or CO	Ni(100)– $p(2 \times 2)$ S + $p(2 \times 2)$ CO rel to	
		Ni(100)– $p(2 \times 2)$ CO	Ni(100)– $p(2 \times 2)$ S
CO total	+0.638	–0.179	
CO 5σ	–0.398	–0.022	
CO $2\pi^*_x$ ^b	+0.746	–0.144	
Co $2\pi^*_y$	+0.449	–0.037	
S total			–0.046
S x,y			–0.028
surface atom ^c	–0.542 (–0.002)	–0.376 (–0.263)	–0.563 (–0.090)
s	+0.004 (–0.005)	–0.120 (–0.034)	–0.039 (–0.001)
z^2	–0.188 (+0.006)	–0.024 (–0.065)	–0.094 (+0.011)
xz^b	–0.262 (–0.087)	–0.190 (–0.091)	–0.337 (–0.063)
yz	+0.010 (–0.024)	–0.109 (–0.089)	+0.016 (+0.002)

^a Net electron gain if positive, loss if negative. ^b Bridging direction along x . ^c Bridged (unbridged).

(100)– $p(2 \times 2)$ S + $p(2 \times 2)$ CO minus that in the single adsorbate system (Ni(100)– $p(2 \times 2)$ S or Ni(100)– $p(2 \times 2)$ CO). A positive value indicates that the coadsorbed species acquires electron density; a negative value indicates a net loss. According to this indicator, the S is more electronegative than 4-fold ortho or bridging CO but more electropositive than 4-fold tetra CO. The results are consistent with the notion that a more electronegative species, the 4-fold CO tetra, will accept more back-bonding.

Although the results thus far are consistent for each site, the question remains as to why these sites behave in fundamentally different ways. Let us begin with the bridging geometry. The arguments for the 4-fold ortho site are much the same.

The composite characteristics of the Ni(100)– $p(2 \times 2)$ S + $p(2 \times 2)$ CO bridging total DOS can be seen clearly in Figure 3. The DOS of the CO and S unsupported nets are represented by bars at the right. In spite of energy

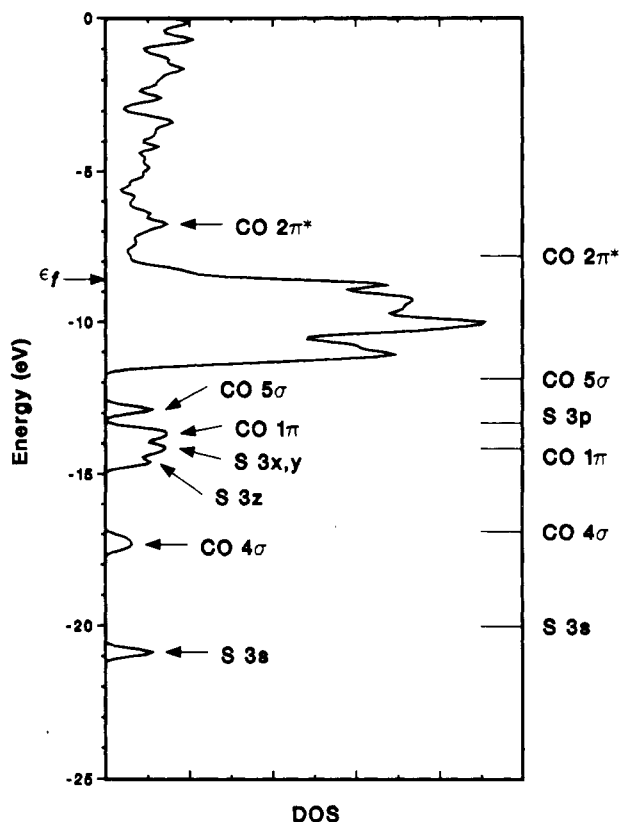
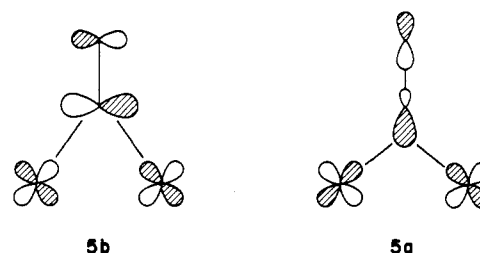


Figure 3. Bridging Ni(100)- $p(2 \times 2)$ S + $p(2 \times 2)$ CO total DOS; major peaks are labeled. The bars on the right indicated the median energies of the CO and S unsupported nets.

shifts, their peakedness is substantially retained; a minimum of 50% of the adsorbate levels fall in their major peaks as labeled. As previously discussed, the direct interaction is predictably small, with $d(\text{C-S}) = 2.78 \text{ \AA}$ and $\text{C-S op} = 0.015$. Some mixing occurs between the CO 1π and the sulfur p levels since they are energetically closely matched. But the 1π is heavily localized at the oxygen end (see Figure 1) and is therefore relatively inert to adsorption. The poisoning must occur via the substrate.

The same conclusions can be drawn from the electron density shifts, of which a selected few are listed in Table V. The excess charge at S is nearly independent of CO adsorption. In contrast, the local surface charge is very much determined by the adjacent surface species. With only one exception, every atom of the initially negatively charged surface (bare Ni(100)) loses electron density as adsorbates are added sequentially. The bridged atoms of the coadsorbed system suffer most with respect to either single species slab.

Let us focus on the xz orbitals, which lie along the bridging direction. As discussed earlier, the electron-withdrawing power of S is felt most strongly at this orbital and its degenerate partner in Ni(100)- $p(2 \times 2)$ S. The largest perturbation of CO adsorption onto either the clean or sulfided surface occurs here as well. The xz is geometrically well suited for interaction with both 5σ and the $2\pi^*_x$, which lies along the bridging direction, depending on the phase relationship between the bridged atoms. The out-of-plane combination can participate in σ -bonding, **5a**, and the in-phase in π -back-bonding, **5b**. The interactions are energetically favored as well. The out-of-phase states will dominate the lower half of the d band (near 5σ) since they are bonding between the metal centers. Likewise, the in-phase set will be concentrated in the upper half, adjacent to the $2\pi^*$. The interaction with the $2\pi^*_x$ is particularly strong; the occupations of the originally degenerate

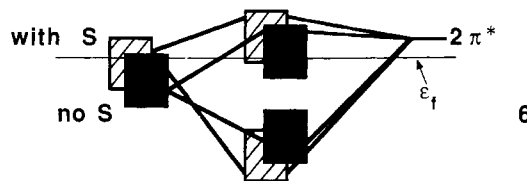


molecular orbitals differ by $0.297e^-$ and the median energies are split by $\sim 1e \text{ V}$. Later, we will use the phase relationships between the Ni atoms and a technique we call COOP to identify the σ and π interacting states.

The stepwise evolution of the xz can be traced in Figure 4. The integral of the projected DOS is compared for Ni(100), Ni(100)- $p(2 \times 2)$ CO, and Ni(100)- $p(2 \times 2)$ S + $p(2 \times 2)$ CO and overlaid onto the total DOS of the latter. The initial localization of the states entirely within the d block is disrupted by both σ and π effects. The mixing is evident from the substantial redistribution of levels into both the 5σ and $2\pi^*_x$ areas. Both effects are magnified with addition of the S adlayer.

If the integrals of the 5σ projected DOS are compared for the surfaces with and without S, we can see that sulfur addition pulls some of the 5σ states into the CO 1π and sulfur p peaks but does not substantially alter either the median of energy or the distribution of levels near ϵ_f . On the other hand, a similar comparison of the $2\pi^*_x$ integrals reveals that the $2\pi^*_x$ level is strongly distorted and the median is pushed up $\sim 1e \text{ V}$. We must remember, however, that these effects cannot be caused by a direct S-CO interaction.

How does the depopulation of the CO $2\pi^*$ come about on the sulfided surface? We saw earlier that the $2\pi^*$ interacts strongly with the upper part of the metal xz band (**5b**). The S p orbitals also interact with the same part of the band and push it up (Figure 4). The metal- $2\pi^*$ interaction becomes stronger since the energy difference is reduced. As a result, both the adsorbate and metal levels are depopulated. To explain why, we turn to the simple two-level interaction diagram used so commonly for molecular systems, and modify it to indicate the inherent level dispersion of infinite systems, **6**. The schematic is crude,



perhaps, but functional nonetheless. The heightened interaction naturally forces upward the resultant antibonding levels, which contain both metal and $2\pi^*$ character. Contrary to molecular systems for which the energy of the HOMO can change due to interactions, the Fermi level of the metal surface is essentially fixed, regardless of the surface species. Our three-layer calculation models this well; the greatest shift of ϵ_f after adsorption is 0.13 eV from the value of the bare surface. The placement of ϵ_f in **6** is crucial. In this case, the arrangement is such that many of the levels are pushed above ϵ_f . A similar interaction in molecular systems will bring about a gain in the occupation of one of the levels at the expense of the other, but here, because ϵ_f is fixed, both metal xz and CO $2\pi^*$ levels lose. An accompanying diagram could be drawn for the CO 5σ interaction with the bottom of the xz band (**5b**). However, most of the levels will lie much below ϵ_f , so that even an interaction of similar magnitude will not alter the 5σ oc-

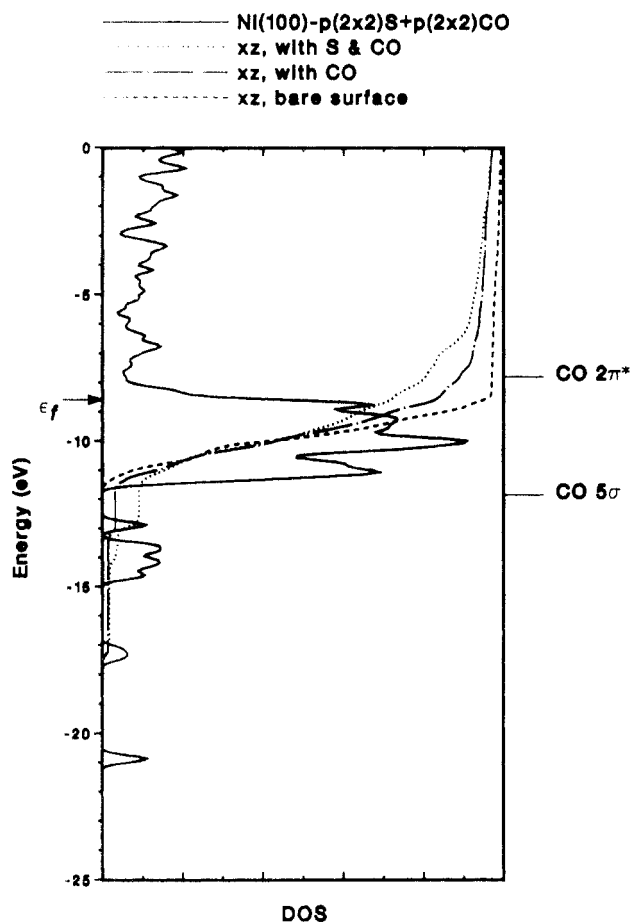


Figure 4. Dashed, dot-dashed, and dotted lines are respectively the integrals of the xz projected DOS of Ni(100), Ni(100)- $p(2 \times 2)$ CO, and Ni(100)- $p(2 \times 2)$ S + $p(2 \times 2)$ CO. The solid curve is the total DOS of the latter. The median energies of the 5σ and $2\pi^*$ coadsorbed levels are indicated on the right.

cupation to the extent of the $2\pi^*$.

Should this interaction, by which S modifies the ability of some surface-localized metal states to bond to the $2\pi^*$ of CO, be called a direct one? We would prefer to refer to it as "through-bond coupling", a concept that has served well in organic^{35a,b} and inorganic^{36a,b} chemistry. Seemingly localized orbitals (lone pairs in two parts of an organic molecule or two metal d orbitals in a binuclear complex connected by one- or many-atom bridges) in two or more parts of a molecule can mix, interact, and split in energy as a result of mixing with orbitals of intervening atoms or groupings of atoms. This is what happens here.

That the 5σ interaction is modified at all can best be followed indirectly through the crystal orbital overlap population (COOP) curve³⁷ of the bridged nickel atoms. The COOP is created by weighing the DOS by its contribution to the Ni-Ni op. In Figure 5, these are compared for the clean and sulfided systems. From 5a and 5b, we know that some Ni-Ni bonding states (near the bottom of the d band) can interact with the 5σ and that some antibonding ones interact with the $2\pi^*$. Indeed, the res-

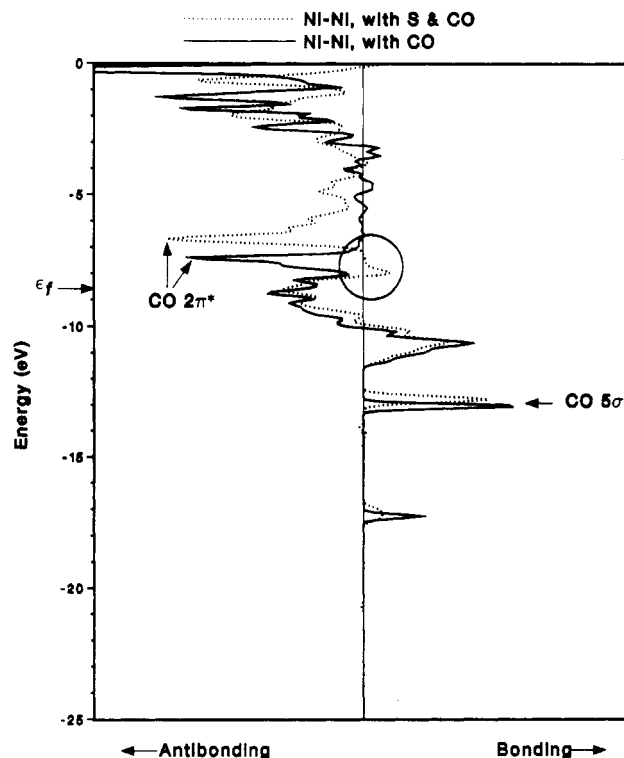


Figure 5. Bridged Ni-Ni COOP's for the Ni(100)- $p(2 \times 2)$ CO and Ni(100)- $p(2 \times 2)$ S + $p(2 \times 2)$ CO are indicated by solid and dotted lines, respectively.

Table VI. Electron Density Changes,^a 4-Fold Tetra CO

atom(s) or orbitals	Ni(100)- $p(2 \times 2)$ CO rel to Ni(100) or CO	Ni(100) $p(2 \times 2)$ S + $p(2 \times 2)$ CO rel to		
		Ni(100)- $p(2 \times 2)$ CO	Ni(100)	Ni(100)- $p(2 \times 2)$ S
CO total	+0.777	+0.064		
CO 5σ	-0.368	+0.009		
CO $2\pi^*$	+0.694	+0.023		
S total				+0.015
S x,y surface atom				+0.005
z^2	-0.283	-0.338	-0.621	-0.266
xy	-0.043	-0.071	-0.114	-0.044
xz, yz	-0.133	-0.023	-0.154	-0.132
	+0.003	-0.129	-0.126	-0.011

^a Net electron gain if positive, loss if negative.

onances with the CO are picked up and the shift from bonding to antibonding through the d block occurs as expected. However, a small bonding region (circled in Figure 5) appears above ϵ_f of the sulfided slab. Assuming conservation of the absolute number of bonding and antibonding states, this packet must have been pushed up from the d block by the sulfur and again by the CO 5σ . Surface levels that should have been filled by σ -donation remain empty. The σ contribution to the chemisorptive bond must be reduced, regardless of the stability of the 5σ occupation. Since the number of affected levels is not substantial, the $2\pi^*$ occupation remains the overriding factor.

Can analogous arguments be used to explain the antiblyholder behavior of the 4-fold tetra system? The charge densities computed for the coadsorbed slab lie much closer to the single species values than do their bridging counterparts. A few are listed in Table VI. That the magnitudes are small should not concern us unduly as the trends tend to be more reliable in similar extended Hückel calculations. Moreover, the trends are consistent among themselves. For example the $2\pi^*$ occupation remains

(35) (a) Grimley, T. B. *Pontif. Acad. Sci., Scr. Varia* 1976, 31, 443; *Proc. Phys. Soc. (London)* 1967, 90, 751. (b) Einstein, T. L.; Schrieffer, J. R. *Phys. Rev. B* 1973, 7, 3629.

(36) (a) Hoffmann, R. *Acc. Chem. Res.* 1971, 4, 1. (b) Gleiter, R. *Angew. Chem.* 1974, 86, 770; *Angew. Chem., Int. Ed. Engl.* 1974, 13, 696.

(37) (a) Shaik, S.; Hoffmann, R.; Fisel, C. R.; Summerville, R. H. *J. Am. Chem. Soc.* 1980, 102, 4555. (b) Whangbo, M.-D. In *Crystal Chemistry and Properties of Materials with Quasi-One-Dimensional Structures*; Rouxel, J., Ed.; D. Reidel: Dordrecht, Holland, 1986; pp 27-85.

(38) Hughbanks, T.; Hoffmann, R. *J. Am. Chem. Soc.* 1983, 105, 1150. Wijeyesekera, S.; Hoffmann, R. *Organometallics* 1984, 3, 949.

Table VII. Extended Hückel Parameters

orbital	H_{ii} , eV	ζ_1	orbital	H_{ii} , eV	ζ_1
Ni 4s	-7.8	2.1	O 2s	-29.6	2.27
4p	-3.7	2.1	2p	-13.6	2.27
3d ^a	-9.9	5.75	S 3s	-20.0	1.817
C 2s	-18.2	1.63	3p	-13.3	1.817
2p	-9.5	1.63			

^a $\zeta_2 = 2.00$; $C_1 = 0.5683$; $C_2 = 0.6292$. C = contraction coefficients used in double- ζ expansion.

directly proportional to the C-Ni_s op and indirectly proportional to the C-O op.

The 4-fold tetra system differs from the others in several respects. It is unique among the coadsorbed systems in that S and CO are each able to withdraw more electron density from the substrate than if adsorbed individually. It is also the only system for which the electronic shifts in the surface levels caused by the coadsorbates are nearly additive. The sum of the charge transfer between the bare and single adsorbate Ni(100) surfaces (columns 2 plus 4 of Table VI) is nearly equivalent to the shifts between the bare and coadsorbed values (column 3). The largest difference is in the degenerate xz and yz orbitals. Individually, S and CO remove a total of $0.122e^-$ from each, but if coadsorbed, $0.014e^-$ more. As a comparison, the greatest discrepancy for the bridged CO systems is nearly 5 times the value (in z^2). In addition, the coadsorbates work on entirely different parts of the surface. This can be seen by comparing the relative charge transfers between coadsorbed and single-species slabs to coadsorbed and bare slabs (columns 2-5 in Table VI). The effect of CO on the clean or sulfided substrate is greatest at the surface xy and smallest at the xz and yz . The reverse is observed for the sulfur modification of the clean or CO-preadsorbed slabs. Thus the adsorption characteristics of either species are nearly independent of the perturbation of surface levels caused by the other. The same information can be obtained by overlaying the appropriate projected DOS curves and integrals.

The answer may lie in the middle layer, rather than the surface. Adsorption of either S, CO, or both will increase the electron density of the bulk layer relative to that of the bare slab. The effect of approximately additive (i.e., the sum of the single species equals coadsorbed system) in every case save the 4-fold tetra site. Here, the electron transfer is slightly more than half as much as expected. A comparison of the bulk atom projected DOS curves uncovers a striking variation in the behavior of the xz and yz on the bulk atom lying immediately below 4-fold coordinated CO. These levels do not interact with $2\pi^*$ of either the single species or the 4-fold ortho coadsorbed system. However, nearly 10% of the xz and yz states are pushed up into the 4-fold tetra $2\pi^*$ peak. In simple terms, an additional metal to CO backbonding interaction has been "turned on", thus the $2\pi^*$ occupation increases. Why is this particular interaction available at this site? It is not due simply to the tetragonal symmetry, since the bulk xz and yz do not interact with $2\pi^*$ in a Ni(100)- $c(2 \times 2)$ CO system. The latter has the same total adsorbate coverage as the coadsorbed systems; each S is simply replaced by an additional CO. We can speculate that the effect of the S on the bulk atom below the 4-fold tetra CO is strong

enough to modify the levels in some way but too weak to constrain their interactions.

Clearly, the mechanisms for interadsorbate interactions are severely limited in this system. Not only does the distance preclude a direct effect, but adsorbate-surface interactions are segregated such that the potential strength of an indirect, substrate-mediated effect is minimized as well. At this point, a good explanation of the trends is still obscure, and we hesitate even to speculate on its origins.

The effect of sulfur on CO adsorption appears to be determined by the interadsorbate distance. At short separations the S and CO, interaction is repulsive—we see site blockage. At intermediate separations, for instance in the energetically favorable geometry where S is in a 4-fold hollow and CO is bridging, we see the workings of the usual Blyholder model. The $2\pi^*$ of CO is populated less, with resultant weakening of C-Ni and strengthening of C-O bonds. We trace this effect to the modification by S of the ability of specific surface orbitals (xz and yz) to back-bond to $2\pi^*$ or through-bond coupling. At longer separations, we see a small reverse effect (C-O weaker, C-Ni stronger) which has some experimental support, but it is easy to rationalize. In general, we think that the simple electronegativity and electron-transfer explanation of coadsorption effects needs to be supplemented by a detailed orbital analysis in terms of through-space and through-bond interactions.

Acknowledgment. We thank Susan Jansen for helpful discussions during the course of this work. This work was supported by the Office of Naval Research.

Appendix

The calculations were performed by using the tight-binding extended Hückel method.^{21a,b} The H_{ii} 's for Ni had been previously determined²⁸ by charge iteration on the bulk metal using Gray's equations.³⁹ The H_{ii} 's for C and O had also been determined previously²⁶ by three-cycle iteration on CO adsorbed onto a four-layer Fe(110) slab. A, B, and C iteration parameters are from ref 38. All parameters, including the uniterated S parameters, are listed in Table VII.

For both the Ni(100)- $p(2 \times 2)$ S and $c(2 \times 2)$ S systems, the Ni-S bond length is reported to be 2.19 Å.³² The Ni(100)- $p(2 \times 2)$ CO geometry is $d(\text{Ni-C}) = 1.80$ Å and $d(\text{C-O}) = 1.15$ Å.^{12c} Adsorbates were placed on one side of the three-layer slab. K point sets of 10 and 16 were used respectively for systems of tetragonal and orthorhombic symmetry. Convergence was checked for 10, 15, and 28 point sets on the Ni(100)- $p(2 \times 2)$ S system. The maximum variations among these sets were 0.007 eV for the Fermi energy, 0.001 eV for the total energy, 0.010 for orbital electron densities, and 0.001 for overlap populations.

Registry No. Ni, 7440-02-0; S, 7704-34-9; CO, 630-08-0.

(39) At $d(\text{Ni-Ni}) = 2.49$ Å, the π bonding interaction is too weak to be detected in the COOP. These levels could interact with one of the CO $2\pi^*$.

(40) Ballhausen, C. J.; Gray, H. B. *Molecular Orbital Theory*; W. A. Benjamin: New York, 1965; p 125.

(41) McGlynn, S. P.; Van Quickenborne, L. G.; Kinoshita, M.; Caroll, D. G. *Introduction to Applied Quantum Chemistry*; Holt, Rinehart and Winston: New York, 1972.